Multidimensional Compactons

Philip Rosenau*
School of Mathematical Sciences, Tel Aviv University, Tel Aviv 69978, Israel

James M. Hyman† and Martin Staley
Theoretical Division, Los Alamos National Laboratory, Los Alamos, New Mexico 87545, USA
(Received 16 March 2006; published 9 January 2007)

We study the two and three dimensional, $N = 2, 3$, nonlinear dispersive equation $C_N(m, a + b)$: $u_t + (u^m)_x + [u^a \nabla^2 u^b]_x = 0$ where the degeneration of the dispersion at the ground state induces cylindrically and spherically symmetric compactons convected in the x direction. An initial pulse of bounded extent decomposes into a sequence of robust compactons. Colliding compactons seem to emerge from the interaction intact, or almost so.

DOI: 10.1103/PhysRevLett.98.024101 PACS numbers: 05.45.Yv, 42.81.Dp, 63.20.Pw, 63.20.Ry

Introduction.—Arguably, modern nonlinear science has started in earnest with the discovery of solitons, c.f. [1]. What started as a humble attempt to understand the FPU and Korteweg–de Vries (KdV) equations has turned into one of the pillars of nonlinear science with a wide range of applications in all fields of physics. However, in spite of many remarkable mathematical advances in the last 40 years the well known solitary structures (whether exactly solitonic or almost so) are mostly limited to one-spatial dimension, 1D [2].

We recall that solitons are a manifestation of a balance between inertial and dispersive forces with soliton supporting equations typically obtained via weakly nonlinear perturbation schemes. However, in higher spatial dimensions these procedures yield equations which typically are not only are nonintegrable but, more importantly, rarely support localized patterns. This, strange at first, phenomenon has a simple explanation: whereas nonlinearity due to inertia plays the same role irrespectively of spatial dimension, the increase in degrees of freedom with dimension, enhances the dispersive spread and thus tilts the balance. Thus a well balanced model in 1D may be less so in a higher dimensions.

For a genuinely localized structure to emerge in N-D naturally rather than as an exception, the dispersive–inertial balance has to be kept irrespectively of spatial dimension. This may be accomplished either by properly enhancing the inertia, see [3], or, as we shall do here, by a proper weakening of the dispersion [4,5]. To this end one has to leave the weakly nonlinear terrain, home of the conventional solitary structures, and probe deeper into the nonlinear zone where a nonlinear dispersion that degenerates at a ground state is found. In 1D this approach begets compactons, robust solitary waves with compact support [5] (see also [6] for a recent exposition). In the present Letter we demonstrate that this mechanism does not depend on dimension and generates N-dimensional compact structures as well, see Figs. 1–9.

The resulting compacton is a robust nonanalytical compact solitary wave with singularity determined by the nonlinearity of the degenerating dispersion, but is independent of its spatial dimension. Notably, compact structures may also form in other, nondispersive, systems with a properly degenerating mechanism [7].

The model equation.—To demonstrate the viability of our arguments, we now present a relatively simple N-D model wherein a unidirectional convection is balanced by a N-dimensional dispersive force [4].

$$C_N(m, a + b): \quad u_t + (u^m)_x + \frac{1}{b}[u^a(\nabla^2 u^b)]_x = 0, \qquad (1)$$

where $m \geq \max(1, a - 1)$ and $b > 0$. As in the 1D model, a particular choice of exponents (m, a, and b) reflects a specific physical mechanism. Thus the $m = 2$, $a = b = 1$ case corresponds to the sedimentation of particles in x direction in a dilute dispersion [8]. Moreover, since for $a = 0$ and $b = 1$ Eq. (1) reduces to the Zakharov-Kuznetsov (ZK) equation [9], it may be viewed as a nonlinear extension of some of the physical mechanisms leading to the ZK, like an evolution of collisionless ion-acoustic waves in a strong magnetic field.

The adopted model is a compromise between a full N-D setup and the available numerical means to study such models, see [4,5], or [10], where a 2D compact breather is presented.

Traveling compactons.—We assume spherically symmetric compactons traversing in x direction. Let

$$s = x - \lambda t \quad \text{and} \quad R = \sqrt{s^2 + y^2 + z^2}. \qquad (2)$$

Integrating in a traveling frame yields

$$u^a\left[-\lambda u^{1-a} + u^{m-a} + \frac{1}{bR^{N-1}}\frac{d}{dR}R^{N-1}\frac{d}{dR}u^b\right] = 0. \qquad (3)$$

Note that λ may be scaled out in terms of $u = \lambda^{m-1}U[\lambda^{m-n/2(m-1)}R]$, where $n \equiv a + b$. Therefore struc-

 © 2007 The American Physical Society

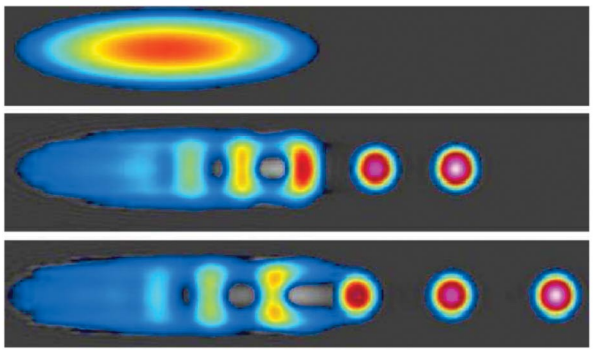

FIG. 1 (color). Position of $C_2(3, 1+2)$ compactons support evolving out of an elongated initial support (upper panel). Their corresponding profiles are displayed on Fig. 2. Note that whenever $m = a + b$ the respective compactons have the same support. Note also that periodic boundaries were assumed.

ture's width scales as $\sim\lambda^{n-m/2(m-1)}$ and as the wave's speed increases its width shrinks (swells), for $m > n$ ($n > m$). When $m = n$, convection and dispersion are in a detailed balance and compactons width is fixed.

Though existence of compactons for Eq. (3) is easily asserted, explicit solutions are not easily deduced. For $N > 1$ we have identified only two types of explicit solutions [4]: (a) $C_N(m = 1 + b, 1 + b)$: The compacton solution is

$$u = \lambda^{1/b}\left[1 - \frac{F(R)}{F(R_*)}\right]^{1/b}, \qquad 0 < R \le R_*, \tag{4}$$

and vanishes elsewhere. In the planar case: $F(R) = J_0(\sqrt{b}R)$ and in 3D: $F(R) = \sin(\sqrt{b}R)/\sqrt{b}R$. In each case integration constant assures that u vanishes at R_*, the first trough of $F(R)$, where it is compactified. (b) $C_N(m = 2, a + b = 3)$: The solution is a parabola

$$u = \kappa_N[\lambda A_N - bR^2], \qquad 0 < R \le R_* \equiv \sqrt{\lambda A_N/b} \tag{5}$$

and vanishes elsewhere. Here

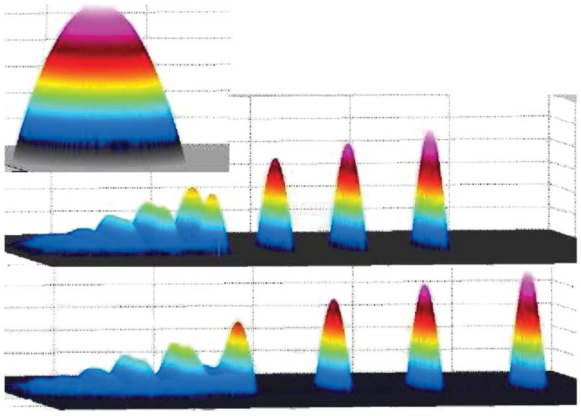

FIG. 2 (color). Temporal snapshots of $C_2(3, 1+2)$ compactons evolving out of an elongated initial pulse (upper panel).

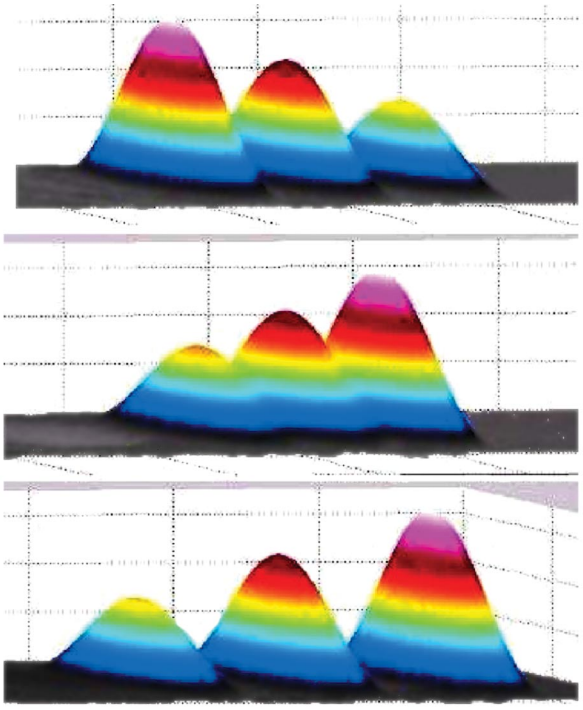

FIG. 3 (color). Collision of three $C_2(2, 0+2)$ compactons with speed $\lambda = 2, 3/2$ and 1. As in 1D, the interaction is very clean and the compactons seem to emerge intact leaving in the perimeter of the domain of interaction a small ripple.

$$C_N(2, 0+3): \quad A_N = \frac{3}{2}(4+N)^2, \ \kappa_N^{-1} = 6(4+N), \tag{6}$$

$$C_N(2, 1+2): \quad A_N = 2(2+N)^2, \ \kappa_N^{-1} = 4(2+N). \tag{7}$$

Note that unlike case (a) now $R_* \sim \sqrt{\lambda}$.

We note the following property of solutions of Eq. (3): given a compacton solution $u(R)$ of $C_N(m, a + b)$, then $V(R) = u^\kappa(R)$ is a solution of $C_N(m_*, a_* + b_*)$ where

$$m_* = 1 + \kappa(m-1), \qquad a_* = 1 + \kappa(a-1), \qquad \text{and} \quad b_* = \kappa b. \tag{8}$$

Thus every solution $u(R)$ generates a κ-parameter family of solutions. However, since $m_* - n_* = \kappa(m-n)$ thus $m \le (>) n$ implies $m_* \le (>) n_*$.

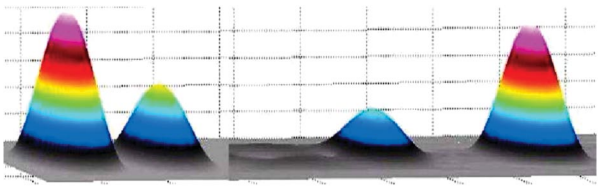

FIG. 4 (color). Collision of two $C_2(2, 1+1)$ compactons corresponding to the sedimentation model [8]. Note the loss of mass of the smaller compacton after the collision. In 2D this effect is more pronounced than in 1D.

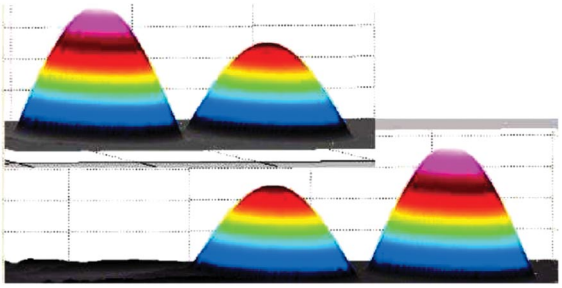

FIG. 5 (color). Display of two colliding $C_2(3, 0 + 3)$ compactons. As in the $C_2(2, 0 + 2)$ case, see Fig. 3, the two compactons reemerge intact after the collision without a measurable loss of mass.

Numerical studies.—The movies of our numerical experiments demonstrate a vastly richer dynamics than in 1D. Each figure is a snapshot of a movie, see [11]. In what follows we describe the essential features of formation and interaction of compactons in 2D. Figures 8 and 9 are a prelude to a more detailed 3D exposition [12].

The essence of our studies is to demonstrate the ability of degenerating nonlinear dispersion to induce robust compact patterns in higher dimensions. Extensive numerical studies which focused on the emergence of compactons out of initial data and their collision, allow us to present a number of meaningful conclusions about (i) the dimension-N and the convection exponent m; (ii) interplay between a and b. The leading dispersive part of (1), $u^{n-1}\nabla^2 u_x$ determines the singularity, but the lower order part, P_*,

$$P_*\colon (u^{n-1})_x\nabla^2 u + (b-1)[u^{n-2}(\nabla u)^2]_x, \qquad (9)$$

plays an essential role in propagation. Its effectiveness is given via $\omega \equiv 1 + b - a$. For a given n, reduction of b reduces ω and the ability of P_* to propel the motion. This is easily seen in Fig. 6 comparing $C_N(2, 0 + 3)$ and $C_N(2, 1 + 2)$: in both we have the same singularity at the edge, in the first case P_* is stronger. We also note that for traveling compactons to emerge we need $\omega > 0$ [4].

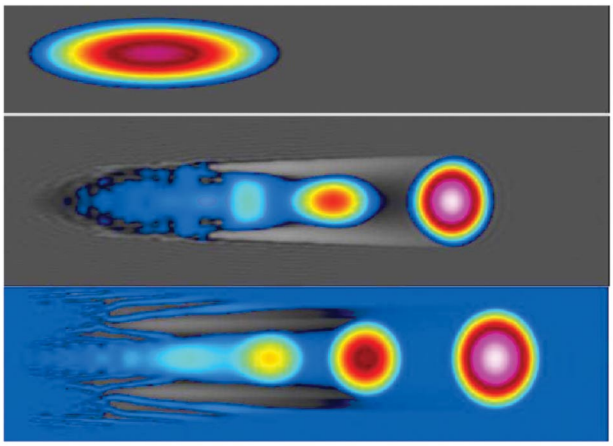

FIG. 6 (color). Evolution of an elongated initial pulse (upper panel) at $t = 18$ for $C_2(2, 0 + 3)$ (lower panel) and $C_2(2, 1 + 2)$ (middle panel). In both cases $n = 3$, but since $b = 3$ and $b = 2$, respectively [see Eq. (8)], in the first case the evolution is faster and the emerging compactons have a wider support.

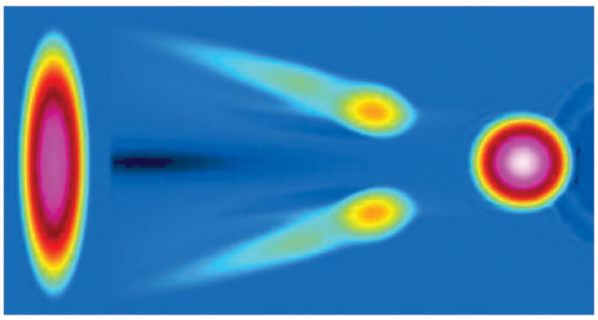

FIG. 7 (color). Decomposition of initial vertical pulse of $C_2(2, 1 + 2)$ into a compacton and a pair of traveling blobs which at a later time coalesce into a second compacton. Unlike Fig. 1 where the initial support stays put while emitting compactons, here the perturbed domain as a whole is in motion.

Emergence of compactons.—See Figs. 1, 2, 6, 7, and 9. In all cases where initial evolution was followed as an initial condition we have used (U_0, α are constants)

$$u = U_0\cos^2(\alpha r), \qquad r \le \frac{\pi}{2\alpha}, \qquad (10)$$

and vanishes elsewhere. The figures show that the number of the emerging compactons and their location depends on the geometry of initial conditions and their span. In Fig. 1 the initial perturbation stays put as it emits compactons. Such a scenario is typical of 1D patterns. On the other hand, emission of compact pulses which are not compactons but converge into compactons as they travel [see Figs. 6 and 9] does not seem to occur in 1D. Also, as seen in Fig. 7, in higher dimensions we observe patterns where the initial pulse propagates as a whole while evolving and emitting compactons.

Interaction between compactons.—Figures 3–5 and 8 present the results of hard collisions that occur when the

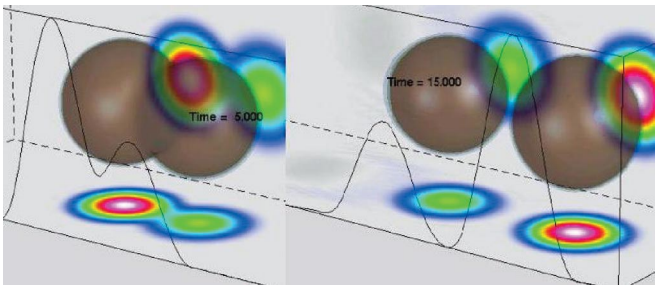

FIG. 8 (color). Collision of two 3D $C_3(2, 0 + 2)$ compactons. Early stage of interaction of their supports at $t = 5$ and immediately thereafter, at $t = 15$. We also project compactons profile $u(R)$.

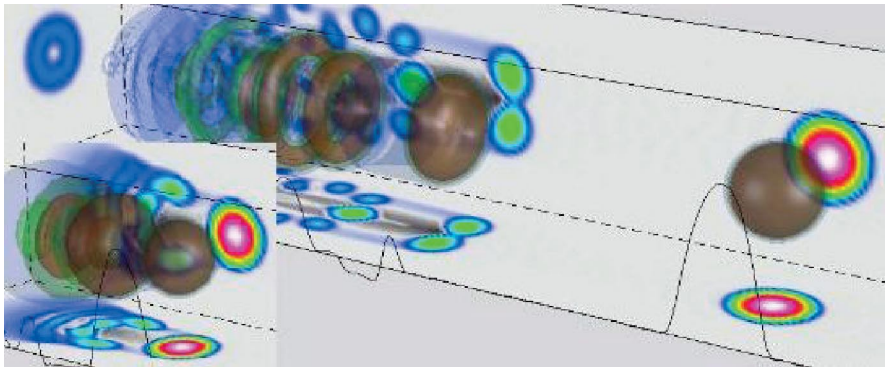

FIG. 9 (color). Emergence of 3D $C_3(2, 0 + 3)$ compactons out of an initial 3D ball which breaks into a sequence of toroidal supports displayed at $t \sim 90$, each of which first turns into a traveling doughnut and later converges into a compacton. The doughnut following the compacton has just emerged. It will converge into a ball at $t \sim 140$. Inset: evolution at $t \sim 25$.

centers of colliding compactons are aligned. Soft collisions, which seem more like a skirmish happen when the center of the faster compacton is off center from its prey. When the centers of softly colliding compactons are sufficiently close, the fast and the slow compactons exchange their positions. As a rule soft collisions seem to be less elastic then their hard counterparts [12].

Some hard interactions appear to be much closer than other to being elastic with the cleanest interaction undoubtedly reserved to the $C_N(2, 0 + 2)$ and $C_N(3, 0 + 3)$ compactons. As in 1D [5], we observe compactons emerging intact in both 2D and 3D cases, see Figs. 3 and 8. In a series of numerical experiments we tested the elasticity of collision between two compactons. An increase in number of modes used begets speeds closer to their precollision values. Though it is unclear that such refinement could be continued indefinitely, we can safely state that the observed interactions are very, very close to being completely elastic.

We also studied $C_2(3, 1 + 3)$ and $C_2(4, 1 + 3)$, not shown. Here even though $m = n$, since $a = 1$, the lower order part (9) is less effective and collisions, though quite clean, are a bit less elastic than in the $m = n$, $a = 0$ cases. While the larger compactons mass is pretty well conserved, after each interaction smaller compactons loose small but a noticeable mass.

The interaction of ''parabolic compactons'' Eq. (5), $m = 2$ and $n = 3$: $C_2(2, 0 + 3)$ and $C_2(1 + 2)$ is far less robust. The smaller compactons reemerge greatly diminished, occasionally accompanied with chunks of splitting off pieces of mass. For a fuller discussion of 3D patterns, see [12].

In conclusion, we have demonstrated that nonlinear dispersion that degenerates at a ground state induces N-dimensional compact robust structures. The studied model, Eq. (1), is a simple example of compacton supporting models. A more general model will be studied in future works.

The work of P. R. (in part), J. M. H., and M. S. was funded by the Department of Energy at LANL under Contracts No. DE-AC52-06NA25396 and the DOE Office of ASCR program in Applied Mathematical Sciences.

*Electronic address: rosenau@post.tau.ac.il
†Electronic address: hyman@lanl.gov

[1] M. D. Kruskal and N. Zabusky, Phys. Rev. Lett. **15**, 240 (1965); M. Ablowitz and H. Segur, *Solitons and the Inverse Scattering Transform* (SIAM, Philadelphia, 1981); P. G. Drazin and R. S. Johnson, *Solitons: An Introduction* (Cambridge University Press, Cambridge, England, 2002).
[2] M. Boiti, J. J. Leon, L. Martina, and F. Pempinelli, Phys. Lett. A **132**, 432 (1988); A. S. Fokas and P. M. Santini, Phys. Rev. Lett. **63**, 1329 (1989); A. S. Fokas, Phys. Rev. Lett. **96**, 190201 (2006); A. S. Kovalev, S. Komineas, and F. G. Mertens, Eur. Phys. J. B **25**, 89 (2002).
[3] P. Rosenau, ''Compact Structures due to Singular Convection or Stress'' (to be published).
[4] P. Rosenau, Phys. Lett. A **275**, 193 (2000); P. Rosenau, Phys. Lett. A **356**, 44 (2006).
[5] P. Rosenau and J. M. Hyman, Phys. Rev. Lett. **70**, 564 (1993); P. Rosenau, Phys. Rev. Lett. **73**, 1737 (1994).
[6] P. Rosenau, Not. Am. Math. Soc. **52**, 738 (2005).
[7] A degeneracy of $u_t = \nabla^2 u^n$ or $u_t = -(u^n u_{xxx})_x$ at $u = 0$, also begets compact patterns. The first describes motion in a porous medium, or diffusion of temperature in plasma. The second—evolution of a viscous drop.
[8] The model equation of sedimentation of dilute suspension is due to J. Rubinstein, Phys. Fluids A **2**, 3 (1990): $u_t + [u(K \otimes u)]_x = 0$. $\otimes$ denotes convolution and the symmetric operator K represents the interacting forces. Expansion in gradients yields Eq. (1) with $a = b = 1$.
[9] V. E. Zakharov and E. A. Kuznetsov, Sov. Phys. JETP **39**, 285 (1974).
[10] P. Rosenau and S. Schochet, Phys. Rev. Lett. **94**, 174102 (2005); P. Rosenau and S. Schochet, Chaos **15**, 015111 (2005).
[11] http://math.lanl.gov/~mac/compacton
[12] J. M. Hyman, M. Staley, and P. Rosenau (to be submitted).